Chapter 4

3D face recognition based on ridge images

In this chapter, we present a method for 3D face recognition from frontal/near-frontal range images based on the ridge lines on the face ~~surface~~. As we discussed in chapter one, the surface matching techniques suffer from computational complexity. In our approach, a subset of points on the face ~~surface~~ are selected using the principal curvature, k_{max}. These points show the locations of the ridge points around the important facial regions on the face, i.e., the eyes, the nose, and the mouth. Instead of matching all ~~of~~ the points on the face surface, the ridge points are used for matching ~~that conducts~~ to huge reduction of the computational complexity ~~of matching~~ while keeping the performance of the system for face recognition promising. We compare the robust Hausdorff distance versus the Iterative Closest Points (ICP) for matching the ridge image of a given probe image to the ridge images of the facial images in the gallery.

4.1 3D face matching based on ridge images

Figure 4.1 shows the block diagram of our method. In the first step, because of noise and artifacts in the range images, we use median filtering and low-pass filtering to remove sharp spikes and smooth the images and then we use interpolation to fill the gaps in the image. In the next step, we roughly find the tip of the nose which is the closest point to the scanner. Because the facial range images in the databases that we work on are frontal/near-frontal, the claim that the tip of the nose is the closest point to the scanner is valid. Then, we apply template matching to localize the face region in the filtered range data. Afterward, we use Gaussian curvature to label three feature points, i.e., the inner corners of the two eyes and the accurate position of the nose tip. We represent the range images by the points on the 3D surface of the face which have maximum principal curvature, k_{max}, greater than a threshold. ~~This representation represents~~ each range image by ridge lines on the 3D surface of the face using a 3D binary image, called ridge image. The detail of preprocessing techniques and 3D facial features labeling were presented in chapter three.
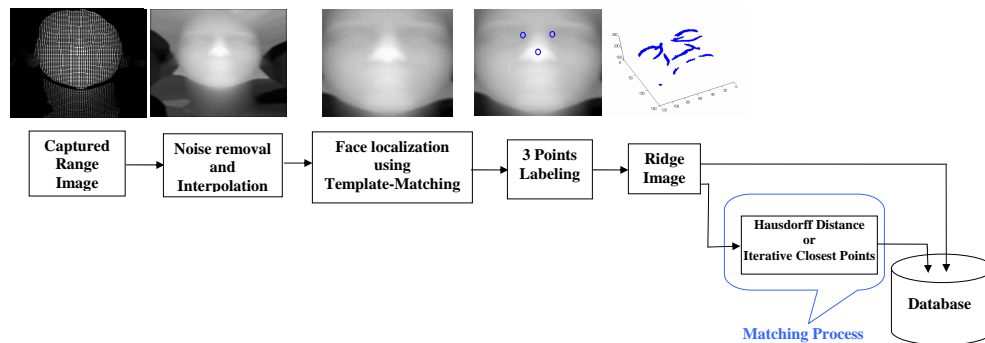

Figure 4.1: *Block diagram of our system for 3D face recognition from range data.*

For recognition, we use two different techniques for ridge image matching: the robust Hausdorff distance and the Iterative Closest Points (ICP). First, we apply similarity transformation (scale, rotation and translation) to find the best pose that matches the probe image with the gallery image. The three labeled feature points plus an auxiliary point in the middle of the triangle formed by the three labeled points are used to find the initial transformation that aligns the probe ridge image to the test ridge image. After initial alignment, for matching based on robust Hausdorff distance, an iterative algorithm is applied to find the optimum pose that results in the minimum Hausdorff distance. For matching based on ICP, we utilized a fast variation of ICP to find the best geometric alignment between a 3D ridge probe image and a given 3D ridge gallery image and compute the Mean Square Error (MSE) distance between the ridge points.

4.2   Ridge image

Our goal is to extract and use the points lying on ridge lines as the feature points. These points correspond to the extreme ridge points on the considered surface. In the literature [13], the ridges are defined as the umbilic points at which the k_{max} attains a local positive maximum. An umbilic point is a point on a surface where the principal curvatures are equal and are non-zero (in the case of zero curvature, the point is called a flat point.) Intuitively, ridges are the points that term the drainage patterns and are called valleys when the ridges are looked from the opposite side.

There are different approaches to locate the ridges [86]. One of the main ap-
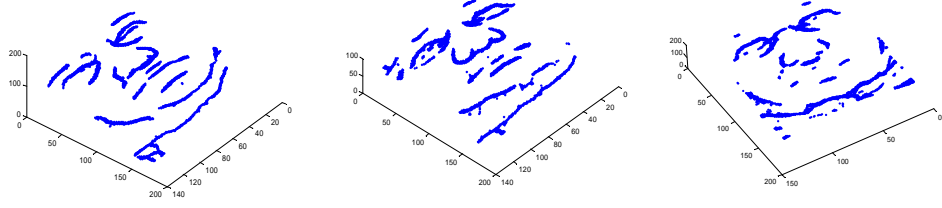
Figure 4.2: *Sample of ridge image extracted for different subjects.*

proaches applies thresholding which is used in this work. We threshold the k_{max} values to find these points. The suitable threshold is obtained based on a small training set that is different from the images in the gallery. The suitable is such that the highest recognition rate for that small training set is achieved. Then, in our experiments the suitable threshold (a fixed value) is used for creating the ridge images for all the facial images in the databases under evaluation. Figure 4.2 shows few examples of the ridge images obtained by thresholding the k_{max} values. These are 3D binary images that show the location of the ridge lines on the surface of the face. The lines on the boundary of the face are filtered out and are not considered as feature points for recognition. To filter out the points on the boundary of the face, we ignore the points on the boundary of the matched template within a margin. In other words, after localizing the face by template matching, the points that are within a certain distance (for example 15 pixels) from the boundary of the matched face template are excluded from the process of ridge creation.

4.2.1 Ridge matching using robust Hausdorff distance

Huttenlocher *et al.* originally proposed Hausdorff distance (HD) [58] as a measure for object matching in computer vision. Unlike other shape matching methods, HD can be calculated without knowing the exact correspondences of the points in different sets. Modifications to the Hausdorff distance raise its capability to handle not only noisy points, but also missing data from occlusion and outliers [59].

Given two sets of points $\mathcal{A} = \{a_1, a_2, ..., a_{N_\mathcal{A}}\}$ and $\mathcal{B} = \{b_1, b_2, ..., b_{N_\mathcal{B}}\}$ of size $N_\mathcal{A}$ and $N_\mathcal{B}$, respectively, the partial Hausdorff distance between the two sets of points $\mathcal{A}$ and $\mathcal{B}$ is defined as:

$$H(\mathcal{A}, \mathcal{B}) = max(h_K(\mathcal{A}, \mathcal{B}), h_K(\mathcal{B}, \mathcal{A})) \tag{4.1}$$

where $h_K(\mathcal{A}, \mathcal{B})$ and $h_K(\mathcal{B}, \mathcal{A})$ represent the directed distance between the two sets $\mathcal{A}$ and $\mathcal{B}$. The directed distances of the partial HD are defined as:

$$h_K(\mathcal{A}, \mathcal{B}) = K_{a\epsilon\mathcal{A}}^{th} d_\mathcal{B}(a), \quad h_K(\mathcal{B}, \mathcal{A}) = K_{b\epsilon\mathcal{B}}^{th} d_\mathcal{A}(b) \tag{4.2}$$

where $d_\mathcal{B}(a)$ represents the minimum distance (e.g. Euclidean distance) value at point a to the point set $\mathcal{B}$, $d_\mathcal{A}(b)$ represents the minimum distance (e.g. Euclidean distance) value at point b to the point set $\mathcal{A}$, $K_{a\epsilon\mathcal{A}}^{th}$ denotes the Kth ranked value of $d_\mathcal{B}(a)$, and $K_{b\epsilon\mathcal{B}}^{th}$ denotes the Kth ranked value of $d_\mathcal{A}(b)$.

After Huttenlocher *et al.*'s original work, researchers have proposed many different definitions and methods to realize directed HD. Dubbisson and Jain revised

the original HD and investigated the performance of 24 different Hausdorrf distance measures based on their behavior in the presence of noise [40]. They proposed the modified Haussdorff distance MHD. Sim *et al.* applied the robust statistic techniques of regression analysis to the computation of the HD measures for object matching, resulting in two robust HD measures: M-HD based on M-estimation and least trimmed square-HD (LTS-HD) based on LTS [126]. Based on the experimental matching performance of these different HD measures, robust LTS-HD based on the least trimmed square (LTS) measure [126] is adopted in our work. In the proposed LTS-HD [126], the directed distance $h_{LTS}(\mathcal{A}, \mathcal{B})$ is defined by a linear combination of order statistics:

$$h_{LTS} = \frac{1}{H} \sum_{i=1}^{H} d_{\mathcal{B}}(a)_{(i)} \tag{4.3}$$

where H denotes $h \times N_{\mathcal{A}}$ ($0 \leq h \leq 1$) as in the partial HD case, and $d_{\mathcal{B}}(x)_{(i)}$ represents the ith distance value in the sorted sequence $d_{\mathcal{B}}(x)_{(1)} \leq d_{\mathcal{B}}(x)_{(2)} \leq \cdots \leq d_{\mathcal{B}}(x)_{(N_{\mathcal{A}})}$. The measure $h_{LTS}(\mathcal{A}, \mathcal{B})$ is calculated by eliminating the large distance values and only keeping the h fraction of the minimum distances. In our experiments, the value of h that resulted in the best recognition rate was 0.8.

In our case, the calculation of LTS-HD is between the two point sets of two 3D binary images, one is the ridge image of the test face image and the other is the ridge image of a gallery face image. The process of finding the best pose between a probe ridge image and a gallery ridge image can be formulated as follows:

$$\arg \min_{\alpha, \beta, \gamma, t_x, t_y, t_z, s} h_{LTS}(Tr(\mathcal{A}), \mathcal{B}) \tag{4.4}$$

(1) Set $\hat{h}_{LTS} := +\infty$, and $t := 0$

(2) Initially align the 3D ridge image of the test image P, i.e. translate, rotate and scale, to the gallery image P', by using the three labeled feature points and the auxiliary point. This similarity transformation is calculated by procrustes analysis [56].

(3) Set $Success := 0$

(4) Place the aligned probe ridge image, $T(P)$, over the gallery ridge image. For all the points in the aligned probe image, find the distance to the closest point in the gallery image, P', using:

$$D_{P'}(x) = min_{y \in P'}||x - y|| \tag{4.5}$$

where the $||.||$ denotes the $L2$ norm.

(5) Sort the minimum calculated distances and then calculate the robust Hausdorff distance, h_{LTS}, using Eq. 4.3.

(6) If $(h_{LTS} <= \hat{h}_{LTS})$, set the following items:

$\hat{h}_{LTS} := h_{LTS}$

$t := t + 1$

$Success := 1$

(7) Change the parameters i.e., translation, rotation, and scale, of the similarity transformation based on the optimization technique. For example, direct search in the simplex method.

(8) If $Success = 1 \ AND \ (t < Max\_Iterations)$ goto 3.

(9) Return h_{LTS}.

Table 4.1: *Iterative algorithm to find the optimum pose in Hausdorff distance matching.*

where $Tr = \begin{bmatrix} sR & T \\ 0^t & 1 \end{bmatrix}$ is a 3D similarity transformation, s is a scale factor, $T = [t_x \ t_y \ t_z]'$ is the 3D translation, and R is a 3D rotation matrix with α, β, and γ as rotation angels.

The process of finding the optimum pose between a probe ridge image and a gallery ridge image is achieved by an iterative approach as shown in table 4.1.

We used the Matlab optimization toolbox, i.e., *fminsearch* Matlab function, to solve this problem. The *fminsearch* uses the simplex search method of [73]. This is a

direct search method that does not use numerical or analytic gradients.

This procedure is repeated to find the matching distance between a probe image and all the images in the gallery. The gallery face image that results in the minimum matching distance, is considered the best match.

4.2.2   Ridge matching using iterative closest points

The ICP algorithm is widely used for geometric alignment of 3D models when an initial estimate of the relative pose is known. Many variants of ICP have been proposed, where the differences are in the phases of selecting, matching the feature points, and/or the minimization strategy. In this work, we use a fast ICP variant [119]. Instead of using random sampling of the feature points as in [119], we use all the feature points in the 3D ridge image in the matching process. Although *random sampling of the points* speeds up the matching process, it has a major effect on the accuracy of the final results.

For the initial alignment of a probe 3D binary ridge image to the 3D ridge images in gallery, the three labeled feature points, i.e., the two inner corners of the eyes and the tip of the nose and an auxiliary point are utilized. Procrustes analysis [56] is then used to estimate the parameters of the similarity transformation (scale, rotation, and translation.) After the initial alignment, we use the aforementioned ICP algorithm to finely align a 3D ridge probe image with a given 3D ridge gallery image and compute the Mean Square Error (MSE) between the points. The smaller the MSE the closer the probe image to the gallery image.

4.2.3 Computational complexity of ridge matching

Compared to other 3D matching approaches for face recognition such as [90, 120, 33], i.e., the second category in our classification, our approach is faster and requires less computations. Obviously, this reduction in computations is due to the fact that we only deal with the ridge lines around the important facial regions on the face, i.e., the eyes, the nose, and the mouth and ignore the surface patches on the face during the matching process. In other words, instead of matching the entire surface of two faces (a probe image and a gallery image), we only match the ridge lines on the face that are detected based on the principal curvature. This reduces the computations in the matching process. In this work, the number of the points in the ridge images that represent the lines around the facial regions are $14\% \pm 2\%$ of the total number of points that cover the face. The computational complexity for both the robust Hausdorff distance and the ICP is $O(PQ)$ with Euclidean distance calculations as the elementary operations, where P and Q are the number of the points in the probe and the gallery. By employing the K-D tree for searching the closest points, the computational complexity is reduced to $O(log(P))$. So, by using the ridge lines, only fraction of the points on the surface of the face are used for face recognition. If we assume that the ridge points are only a fraction, i.e., $\rho < 1$, of the entire points on face surface, e.g., 0.14 ± 0.02 in our work, then the computational complexity reduces to $\rho^2 O(PQ)$ for the regular scheme and to $O(log(P) - log(1/\rho))$ for the accelerated scheme. This means that by using the ridge points, the computational complexity of matching is reduced an order of magnitudes.

4.2.3   Computational complexity of ridge matching

Compared to other 3D matching approaches for face recognition such as [90, 120, 33], i.e., the second category in our classification, our approach is faster and requires less computations. Obviously, this reduction in computations is due to the fact that we only deal with the ridge lines around the important facial regions on the face, i.e., the eyes, the nose, and the mouth and ignore the surface patches on the face during the matching process. In other words, instead of matching the entire surface of two faces (a probe image and a gallery image), we only match the ridge lines on the face that are detected based on the principal curvature. This reduces the computations in the matching process. In this work, the number of the points in the ridge images that represent the lines around the facial regions are $14\% \pm 2\%$ of the total number of points that cover the face. The computational complexity for both the robust Hausdorff distance and the ICP is $O(PQ)$ with Euclidean distance calculations as the elementary operations, where P and Q are the number of the points in the probe and the gallery. By employing the K-D tree for searching the closest points, the computational complexity is reduced to $O(log(P))$. So, by using the ridge lines, only fraction of the points on the surface of the face are used for face recognition. If we assume that the ridge points are only a fraction, i.e., $\rho < 1$, of the entire points on face surface, e.g., 0.14 ± 0.02 in our work, then the computational complexity reduces to $\rho^2 O(PQ)$ for the regular scheme and to $O(log(P) - log(1/\rho))$ for the accelerated scheme. This means that by using the ridge points, the computational complexity of matching is reduced an order of two magnitudes.

4.3 Experiments and results

We use the Gavab database [97] and the FRGC V2.0 [114] 3D face databases for our experiments. In the following subsections we review these two databases and present our experiments and results.

4.3.1 Experiments on Gavab database

As described in Section 3.4, the Gavab database contains range images of 61 subjects. In our experiments, we used the two neutral frontal images (the 1st and the 2nd captures), the two neutral looking up and down images (the 5th and the 6th captures), the frontal images with smile expression (the 7th capture), the frontal images with laughing expression (the 8th capture), and a frontal image with random gesture (the 9th capture). The images in the 2nd capture are used as gallery images and the images in the $1^{st}, 3^{rd}, 4^{th}$, and $7-9^{th}$ captures are used as the probe images for recognition.

Figure 4.3 shows three samples of the original images in the Gavab database, results of noise removal and interpolation, face localization, feature points labeling, and ridge images.

For recognition, we compared between the robust Hausdorff distance and the ICP techniques. Table 4.2 presents the results of the experiments. For neutral frontal images, only four subjects out of 61 subjects were not identified by both algorithms (93.5% rank-one identification rate). In another experiment, we projected the frontal ridge images to 2D (ignoring the 3rd dimension) and the recognition process was tested. By ignoring the 3rd dimension, we obtained rank-one identification rate of
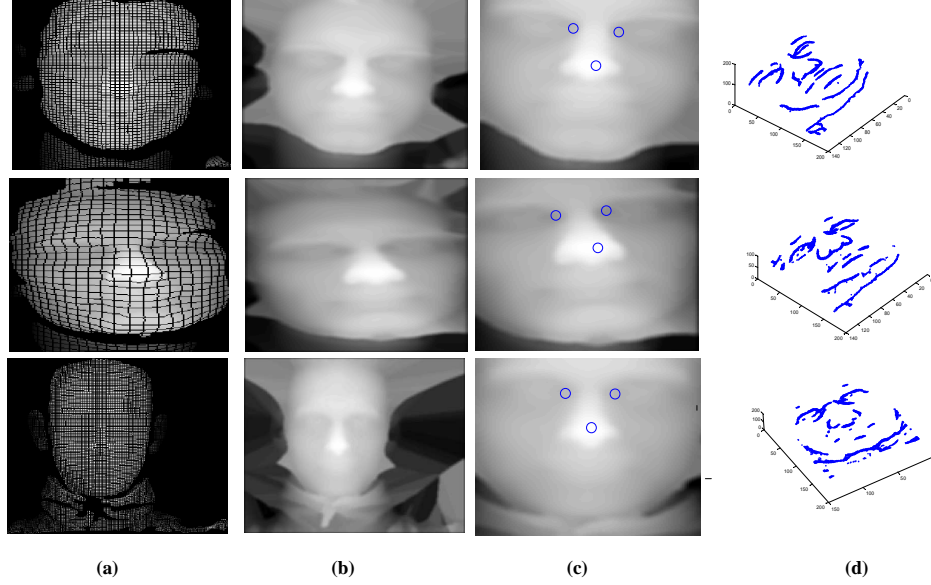
Figure 4.3: *Samples of range images in the gallery and the results of preprocessing (a) Original range images, (b) Noise removal and interpolation, (c) Face localization and three feature points labeling, (d) Ridge images*

82.0% and 86.9% using robust Hausdorff distance and ICP, respectively. This result supports the opinion that 3D data has more potential for face recognition than 2D data.

For faces with expressions, we considered only the upper part of the face, i.e., the 3D ridge lines around the eyes and the nose, for recognition and excluded the lower part of the face, i.e., the mouth, which is affected by the expression. We achieved a recognition rate of 83.6% using the ICP technique and 82.0% using the robust Hausdorff distance for the smiling expression.

Furthermore, we evaluated the performance of our approach for recognition of facial images with pose (looking up/down) based on both the ICP and the robust Hausdorff distance techniques. The recognition rates for the facial images with the

Facial Expression	1st Rank Recognition (%)	
	Robust H.D.	ICP
Neutral (3D)	93.5	95.0
Smiling (3D)	82.0	83.6
Laughing (3D)	73.8	68.9
Random Gesture (3D)	63.4	63.4
Looking Up (3D)	75.4	88.6
Looking Down (3D)	70.5	85.3

Table 4.2: *Results of first-ranked recognition rate on the Gavab face database using range data.*

looking up (down) pose are 88.6% (85.3%) and 75.4% (70.5%) using the robust Hausdorff distance and the ICP technique, respectively.

Figure 4.4 and 4.5 show the performance of the system in term of Cumulative Match Characteristic (CMC) curve and Receiver Operating Characteristic (ROC), respectively, for the neutral versus neutral frontal facial images using the ICP and the robust Hausdorff distance matching techniques. Our experiments show that the performance of ICP and the robust Hausdorff distance are comparable and ICP slightly outperforms the robust Hasudorff distance (except for the laughing expression).

We compared our algorithm with three different approaches for 3D face recognition that were presented by Moreno *et al.* in [100, 99, 98] based on the Gavab dataset. In [100], they segmented the range images into isolated subregions using the mean and the Gaussian curvatures. Then, they extracted 86 descriptors such as the areas, the distances, the angles, and the average curvature of the subregions. They selected 35 best features and utilized them for face recognition based on the minimum Euclidean distance classifier. They achieved a first ranked recognition rate of 78.0% for neutral frontal images and 62% for images with smile expression (only 60 subjects out 61
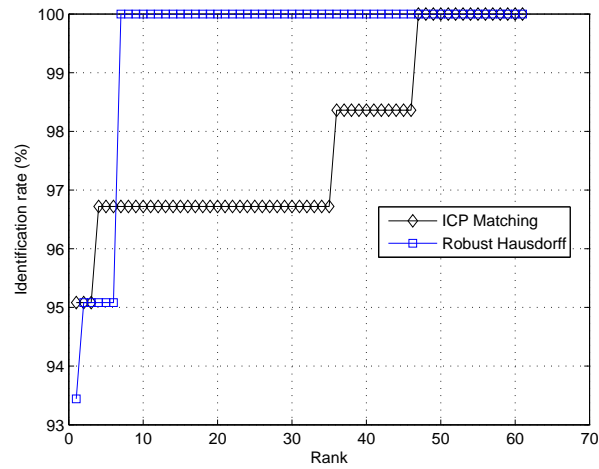
Figure 4.4: *CMC curves for frontal neutral images in Gavab database based on ridge images matched using the ICP and Hausdorff distance techniques.*
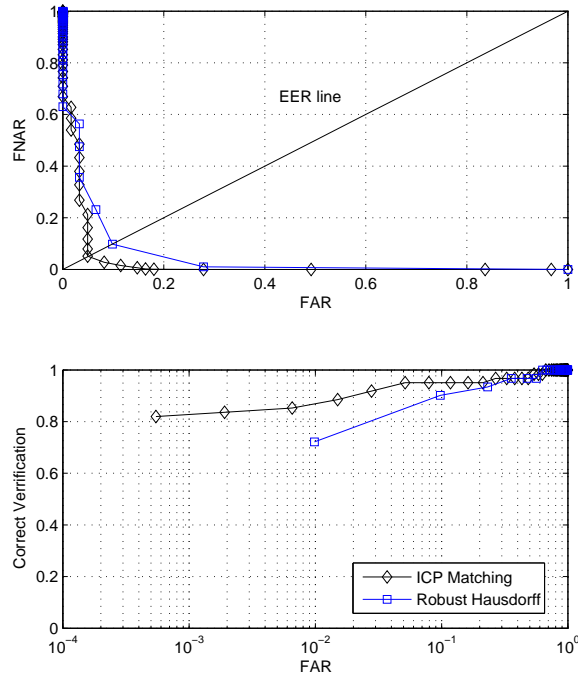

Figure 4.5: *ROC curves for frontal neutral images in Gavab database based on ridge images matched using the ICP and Hausdorff distance techniques.*

Approach	Neutral-Neutral%	Neutral-Pose/Expr.%	Technique
Moreno *et al.* [100]	78.0	62.0	35 features(e.g., areas of subregions)
Moreno *et al.* [99]			
	82.0	76.2	30 features and PCA
	90.16	77.9	30 features and SVM
Moreno *et al.* [98]	90.16	77.9	3D volxels
Our results	93.5	75.4/82.0	Robust Hausdorff distance
	95.0	88.6/83.6	Iterative Closest Points

Table 4.3: *Comparing the results by Moreno et al. [100, 99, 98] on Gavab database and our work.*

from the database were utilized). In [99], they selected a set of 30 features out the 86 features and obtained recognition rates of 82.0% and 90.16% when the images are frontal views with neutral expression using Principal Component Analysis (PCA) and Support Vector Machines (SVM), respectively. The recognition rates decreased to 76.2% and 77.9%, using PCA and SVM matching schemes, respectively, when using probe images with expressions and slight face rotation. In [98], the authors represented the face using 3D voxels. Experiments were performed on both images with neutral expression and images with either pose variations or facial expressions. The best recognition rate that they achieved was 90.16% for the images with neutral expression and 77.9% for the images with pose and facial expressions. Table 4.3 summaries their results as well as ours. As the results show, our method based on ridge images and ICP technique for matching has a better recognition performance for images with neutral expression, with expressions, and with poses.

4.3.2 Experiments on FRGC V2.0 face database

The FRGC V2.0 database [114] consists of 50,000 recordings divided into training and validation partitions. The training partition is designed for training algorithms and the validation partition is for assessing the performance of a system in a laboratory setting. FRGC V2.0 consists of six experiments, where the third experiment measures the performance of 3D face recognition. In the third experiment, the gallery and probe data sets consist of both range and texture images for each subject. The 3D images were acquired by a Minolta Vivid 900/910 series sensor. There are 4007 pairs of images (range and texture) for 466 subjects in the validation set. The set contains images from 1 to 22 sessions per subject, including images with neutral expression and images with other expressions. 370 subjects have at least two ~~neutral~~ images and 432 subjects have at least one neutral image. Figure 4.6 shows few samples of range images along with the range data for different subjects in the FRGC V2.0 database.

We investigated the performance of our algorithm on the neutral 3D face images of the FRGC V2.0 database. First, we compared the performance of the robust Hausdorff distance and the ICP technique for matching the ridge images. There are 370 subjects that have at least two neutral images captured in different sessions. For some of the subjects, there are more than two captured neutral images with a time laps of one week between them. We chose the two farthest captured images for each subject and considered the oldest one as the gallery and the most recent captured as the probe. The result of rank-one identification using the robust Hausdorff distance on this selected dataset is 41.62% while the result of the ICP technique for matching

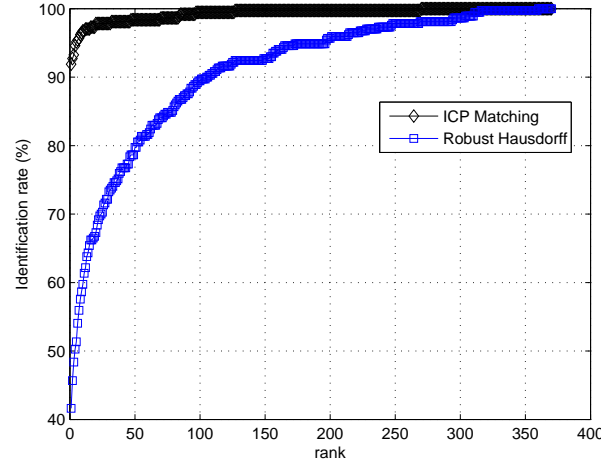Figure 4.6: *Samples of facial images in the FRGC V2.0 database (texture, range, and extracted ridge images.)*

Figure 4.7: *CMC curve for 370 subjects in the FRGC V2.0 database based on ridge images matched with the ICP and Hausdorff techniques.*

is 91.8%. This means that with the ICP based matching approach not only the best performance is achieved, but also it is robust with the increase in the size of the database. To remind the readers, for a small size database such as Gavab, the performance of the Hausdorff matching and the ICP matching were comparable (ICP was slightly better.) This lesson is also learned from Yan and Bowyer in [142], where they compared ICP and Hausdorff for ear surface matching. Their experiments support our results that the ICP outperforms the Hausdorff distance for shape matching.

Figure ?? shows the CMC curve for 370 subjects in the FRGC V2.0 database

4.3.3 Comparison between the ridge points, random points selection, and entire face surface

In order to justify that the ridge points are the important points on the face for 3D face matching, we experimented 3D face recognition using random selection of the

Database	Ridge Points	Random Points	Complete Surface
Gavab (61 subjects)	95.0	67.2	95.0
FRGC V2.0 (370 subjects)	91.8	10.0	97

Table 4.4: *Comparison between the ridge points, random points selection, and entire surface based on the ICP matching technique; Results are in term of rank-one identification rate (%).*

points on the entire face surface and matching them with the ICP method. A set of random points were selected from the range images such that the x and y points are randomly selected using a random generator with uniform distribution and the z values of each point come from the existing depth values of the probe and the gallery image. The number of the random points is as the average number of the ridge points in the ridge image. Then, these random points are used for matching based on the ICP technique. In addition we used all the points on the face surface for matching based on the ICP technique. The results of these experiments are summarized in table 4.4 for the data GavabDB and FRGC V2.0.

The result of our experiment shows that the ridge points are robust for 3D face recognition versus random point selection for matching. Specially, when the size of the database is large enough (370 subjects in FRGC V2.0), the performance of matching based on random points selection is very low (10% for the FRGC V2.0 dataset.) Compared to the matching scheme using all the surface points, as long as the size of the database is small, the ridge points full points have the same performance. With increasing in the size of the database, the recognition rate does not drop significantly (91.8% compared to 97% on the FRGC2.0 dataset.) In conclusion, there is a tradeoff

between the performance and computational complexity in shape matching and our experiments show that ridge points are very promising in surface matching. In other words, ridge points have good performance rate while reducing the computational complexity of matching an order of two magnitudes.

4.3.4   More results on FRGC2.0

In another experiment, we evaluated the capability of the ridge images for face verification on FRGC V2.0 face database. Since ICP has a better performance than robust HD technique for matching, only the ICP technique is used in the rest of our experiments. Figure 4.8 shows the result of the verification experiment for the neutral facial images (total of 2365 facial images for 432 individual subjects). The results are presented as ROC curve. As the ROC curve shows the performance of 3D face recognition based on ridge images and the ICP technique for matching is 88.5% verification at 0.1% False Acceptance Rate (FAR). Table 4.5 breaks down the results of the 3D for verification at 0.1% FAR in terms of three different ROCs. In ROC I all the data are within the semesters (Fall 2003 and Spring 2004), in ROC II the data are within the year, and in ROC III the images are between the semesters (see Figure 4.9). This means that the experiment that produced ROC III is the toughest experiment. The table represents the results of verification for neutral v.s. neutral images in FRGC V2.0 dataset (2365 images of 432 subjects). The last column of the table shows the results of the FRGC baseline for the three ROCs. The baseline algorithm for the 3D scans in FRGC consists of PCA performed on the shape and texture
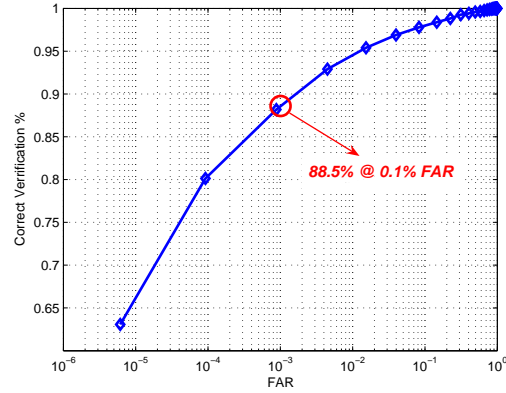
Figure 4.8: *ROC curve for the neutral faces versus neutral in FRGC2.0 database (total of 2365 facial images for 432 individual subjects); ICP technique is used for matching the ridge images.*

Neutral	3D (%)	FRGC Baseline (%)
ROC I	90.69	90.00
ROC II	88.5	86.01
ROC III	85.75	81.58

Table 4.5: *Verification rates (%) at 0.1% FAR for the ROC I, II, and III of the neutral v.s. neutral images.*

channels separately and then fused. Compared to the FRGC baseline, our approach has a better performance. Furthermore, comparison between our results in the three ROCs, shows that the performance of our system does not drop significantly under the effect of aging and time laps between the captured sessions. This validates our claim that the ridge lines have great potential for face recognition under the effect of aging.
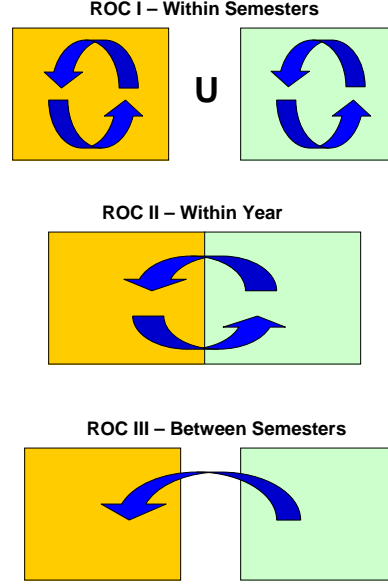
ROC I – Within Semesters

ROC II – Within Year

ROC III – Between Semesters

Figure 4.9: *ROC I: the data are within the semesters. ROC II: the data are within the year. ROC III: the images are between the semesters.*

4.4   Summary

In this chapter, we have presented an approach for 3D face recognition from frontal range data based on the ridge lines on the face surface. We have used the principal curvature, k_{max}, to represent the face image as a 3D binary image called ridge image. The ridge image shows the locations of the ridge points around the important facial regions on the face, i.e., the eyes, the nose, and the mouth. We have utilized the robust Hausdorff distance and the Iterative Closest Points (ICP) for matching the ridge image of a given probe image to the ridge images of the facial images in the gallery. To test the performance of our approach for 3D face recognition, we have performed experiments on GavabDB face database (a small size database) and Face Recognition Grand Challenge V2.0 (a large size database). The results of the experiments have

shown that the ridge lines have great capability for 3D face recognition. In addition, we have found that as long as the size of the database is small, the performance of the ICP based matching and the robust Hausdorff matching are comparable. But, when the size of the database increases, ICP based matching outperforms the robust Hausdorff matching technique.